DOI: 10.1002/ejic.201000324

Dual Luminescent Dinuclear Gold(I) Complexes of Terpyridyl-Functionalized Alkyne Ligands and Their Efficient Sensitization of Eu^{III} and Yb^{III} Luminescence

Xiu-Ling Li,*[a] Ke-Juan Zhang,[a] Juan-Juan Li,[a] Xin-Xin Cheng,[a] and
Zhong-Ning Chen[b]

Keywords: Gold / Lanthanides / Dinuclear complexes / Sensitized luminescence / Alkynes

Reaction of $(tpyC_6H_4C{\equiv}CAu)_n$ {$tpyC_6H_4C{\equiv}CH$ = 4′-(4-ethynylphenyl)-2,2′:6′,2′′-terpyridine} with diphosphane ligands $Ph_2P(CH_2)_xPPh_2$ (x = 2 dppe, 3 dppp, 4 dppb, 5 dpppen, 6 dpph) in CH_2Cl_2 afforded the corresponding dual luminescent binuclear gold(I) complexes $[(tpyC_6H_4C{\equiv}CAu)_2(\mu\text{-dppe})]$ (**1**), $[(tpyC_6H_4C{\equiv}CAu)_2(\mu\text{-dppp})]$ (**2**), $[(tpyC_6H_4C{\equiv}CAu)_2(\mu\text{-dppb})]$ (**3**), $[(tpyC_6H_4C{\equiv}CAu)_2(\mu\text{-dpppen})]$ (**4**), $[(tpyC_6H_4C{\equiv}CAu)_2(\mu\text{-dpph})]$ (**5**). Crystal structural analysis of complexes **1**·$2CH_2Cl_2$ and **2**·$2CH_2Cl_2$ show that the terpyridine moieties are free of coordination in these gold(I)-acetylide-phosphane complexes. Spectrophotometric titration between complex **1** and $[Eu(tta)_3]$ (Htta = 2-thenoyltrifluoroacetone) or $[Yb(hfac)_3(H_2O)_2]$ (Hhfac = hexafluoroacetylacetone) gave a 2:1 ratio between Ln(β-diketonate)$_3$ (Ln = Eu, Yb) units and the complex **1** moiety, indicating the formation of Au_2Ln_2 complexes. Both the luminescence titrations and the luminescence quantum yields of Au_2Ln_2 (Ln = Eu, Yb) solutions show that the energy transfer occurs efficiently from the binuclear gold(I) antennas **1**–**5** to Eu^{III} and Yb^{III} centers, and all complexes **1**–**5** are good energy donors for sensitization of visible and NIR luminescence of Eu^{III} and Yb^{III} ions.

Introduction

Lanthanide(III) luminescence has attracted intensive research efforts because of its distinct advantages such as high color purity induced by narrow emission bands, long radiative lifetimes of the excited states in the range of microseconds to milliseconds, large Stokes' shifts, and relatively immovable emission positions.[1–2] Because of these advantages, lanthanide(III) complexes have been extensively applied to biomedical assays, optical communication, magnetic resonance imaging, lasers, and as components of the emitter layers in multilayer organic light-emitting devices (OLEDS), etc.[3–5] But direct excitation of the Ln^{III} centers always leads to inefficient luminescence because of the extremely weak absorption from Laporte-forbidden f-f transitions of the Ln^{III} ions.[1b] In order to improve the luminescence yields of Ln^{III} ions, one of the most feasible strategies is to use strong absorbing organic or d-block metallorganic antenna chromophores as ligands and sensitizers.[2a,6–8] Ln(β-diketonate)$_3$ moieties represent another efficient and well-investigated type of Ln^{III} co-ordinating unit. The two coordinated water molecules in $[Ln(\beta\text{-diketonate})_3(H_2O)_2]$ compounds can be easily replaced by chelating chromophores such as phenanthroline or polypyridine, which results in highly luminescent ternary complexes.[6–7,8a,9]

With respect to energy-transfer processes and minimization of nonradiative deactivation in the d-f assembly, it is very advantageous to use polypyridine-functionalized alkynyl ligands to assemble d-f arrays because they contain both soft donors in the alkynyl positions and hard donors in the polypyridine moieties.[6–7,8a] The polypyridine unit can provide high coordination number and eliminate water molecules from the first coordination sphere of Ln^{III} centers effectively because of its good chelating ability. On the other hand, the good linearity and conjugacy of polypyridine-functionalized alkynyl ligands are favorable to the energy transfer from the antenna ligand to the Ln^{III} luminescence centers.[6–7,8a] A series of polypyridine-functionalized alkynyl ligands were utilized for the construction of d-block chromophores by incorporation with $[Ln(\beta\text{-diketonate})_3(H_2O)_2]$ compounds achieving sensitized lanthanide luminescence in our previous work.[2a,6–7]

Other important effects in achieving efficient energy transfer from the antennas to Ln^{III} (Ln = Eu, Yb) centers include the energy match between the triplet state and the $^5D_0$ energy level of the Eu^{III} ions,[9b,10] and the overlap degree between the emission bands of the antennas and the absorption spectra of Yb^{III}.[6] So whether the triplet states of the antennas can be determined easily, especially at room temperature, becomes very important to avoid a blind at-

---

[a] School of Chemistry and Chemical Engineering, Xuzhou Normal University,
Xuzhou, Jiangsu 221116, China
E-mail: lxl@fjirsm.ac.cn
[b] State Key Laboratory of Structural Chemistry, Fujian Institute of Research on the Structure of Matter, Chinese Academy of Sciences,
Fuzhou, Fujian 350002, China

Supporting information for this article is available on the WWW under http://dx.doi.org/10.1002/ejic.201000324.

tempt. The organometallic Au^I phosphane acetylides have exhibited easily observed phosphorescence emission properties due to the heavy atom effect of the Au^I ions or aurophilic interactions,[7d,11–14] so that their triplet states can be easily concluded. In addition, their long phosphorescence lifetimes favor energy transfer.[6,7,11d,12b,14b] It has been reported that the Au^I acetylide phosphane chromophores are favorable antenna chromophores for sensitization of lanthanide luminescence when using 5-ethynyl-2,2′-bipyridine as a bridging ligand in the Au_4Ln_4 or Au_2Ln_2 complexes, but the reported quantum yields of Eu^{III} complexes are relatively low (0.010–0.012),[7d] and the triplet states of the antennas in dichloromethane solutions could not be observed at room temperature. In order to obtain an intensely phosphorescent system at room temperature, and understand further how to better match the triplet states of gold(I) antennas and the emitting levels of Ln^{III} and figure out which Ln^{III} ions may be sensitized efficiently, the conjugated degree of the alkyne system should be more extended because most phosphorescent systems at room temperature have a large conjugated degree apart from the heavy atom.[6,7d,11,14b] On the basis of this consideration, the terpyridyl-functionalized alkyne ligand 4′-(4-ethynylphenyl)-2,2′:6′,2′′-terpyridine ($tpyC_6H_4C\equiv CH$) is a judicious choice, and a series of its intense room temperature phosphorescent Pt^{II} complexes have been synthesized and used as efficient sensitized chromophores in our previous work.[6] For this work a series of binuclear gold(I)-alkynyl-phosphane complexes were prepared by depolymerization of polymeric $(tpyC_6H_4C\equiv CAu)_n$ with diphosphane ligands $Ph_2P(CH_2)_xPPh_2$ (x = 2 dppe, 3 dppp, 4 dppb, 5 dpppen, 6 dpph) in CH_2Cl_2. The luminescence titrations and luminescence quantum yields of Au_2Ln_2 (Ln = Eu, Yb) solutions demonstrate that all complexes **1**–**5** are good energy donors for sensitization of visible and NIR luminescence of Eu^{III} and Yb^{III} ions.

Results and Discussion

Syntheses of Gold(I) Complexes and Characterization

The dinuclear gold(I)-phosphane-acetylide complexes were prepared by general methods established previously[7d] through the reaction of diphosphane ligands with the corresponding gold(I) coordination polymer $(tpyC_6H_4C\equiv CAu)_n$ (Scheme 1) and purified by chromatography on short silica-gel columns using dichloromethane/methanol (100:2) as eluent. Recrystallization was carried out through slow diffusion of *n*-hexane into the corresponding concentrated dichloromethane solutions, from which pale yellow crystals of complexes **1**·$2CH_2Cl_2$, and **2**·$2CH_2Cl_2$ suitable for X-ray diffraction were obtained. In the IR spectra, all the dinuclear gold(I)-phosphane-acetylide complexes **1**–**5** exhibit $\nu_{C\equiv C}$ modes at about 2110 cm^{-1}, which falls into the normal range of terminally σ-coordinated alkynyl ligands.[6,7] Lower frequency for the $\nu_{C\equiv C}$ bands is not observed, indicating no π-coordination mode of the C≡C bond exists.[6,7,15–17]

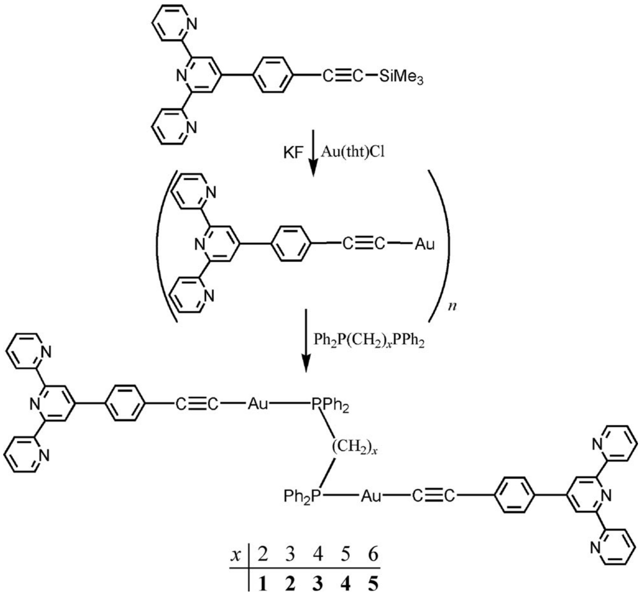

Scheme 1. Synthetic routes to complexes **1**–**5**.

Crystallographic Studies

The crystal structures of **1**·$2CH_2Cl_2$ and **2**·$2CH_2Cl_2$ were determined by single-crystal X-ray diffraction. Selected bond lengths and angles are presented in Table 1. The molecular structures of **1**·$2CH_2Cl_2$ and **2**·$2CH_2Cl_2$ are shown in Figures 1 and 2, respectively. Complexes **1**·$2CH_2Cl_2$ and **2**·$2CH_2Cl_2$ crystallize in the triclinic system with space group $P\bar{1}$ and monoclinic system with space group *C*2/*c*, respectively. Complex **1**·$2CH_2Cl_2$ adopts a *trans* conformation. Complex **2**·$2CH_2Cl_2$ adopts a *gauche* conformation with a P1–C71–C72–C71A torsion angle of 175(2)°. The Au^I centers in the two complexes adopt quasilinear coordination geometries as reported in many gold(I)-acetylide-phosphane complexes,[11–14,17–19] and the C–Au–P angles are in the range of 177.2(4)–178.5(2)°, deviating slightly from 180°. The bond lengths of Au–P [2.271(2)–2.282(4) Å] and Au–C [1.971(12)–2.027(6) Å] are in good agreement with the lengths in analogous Au-acetylide systems.[11–14,17–20] The C≡C distances [1.162(10)–1.224(15) Å] are comparable to those in the similar dinuclear gold(I)-arylacetylide-phosphane complexes.[20] The intramolecular Au···Au distances are 7.078 Å in **1**·$2CH_2Cl_2$ and 5.294 Å in **2**·$2CH_2Cl_2$, while the closest intermolecular Au···Au distances are 8.840 Å in **1**·$2CH_2Cl_2$ and 6.556 Å in **2**·$2CH_2Cl_2$.

Table 1. Selected bond lengths [Å] and angles [°] for **1**·$2CH_2Cl_2$ and **2**·$2CH_2Cl_2$.

1·$2CH_2Cl_2$		**2**·$2CH_2Cl_2$	
Au–P1	2.271(2)	Au1–P1	2.282(4)
Au–C23	2.027(6)	Au1–C1	1.971(12)
C22–C23	1.162(10)	C1–C2	1.224(15)
C23–Au–P1	178.5(2)	C1–Au1–P1	177.2(4)
C22–C23–Au	175.5(8)	C2–C1–Au1	173.8(11)
C19–C22–C23	178.7(8)	C3–C2–C1	179.4(14)

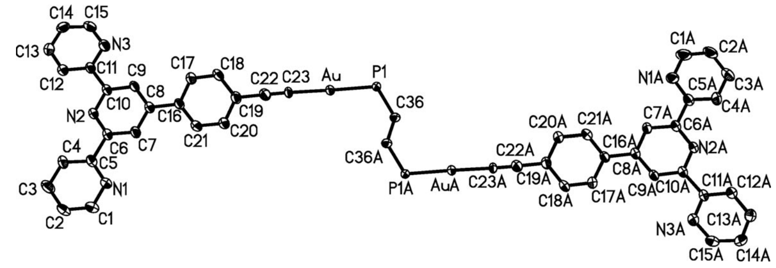

Figure 1. ORTEP drawing of **1**·2CH$_2$Cl$_2$ with atom labeling scheme showing 30% thermal ellipsoids. Phenyl rings of dppe, CH$_2$Cl$_2$ molecules, and hydrogen atoms are omitted for clarity (symmetry code for A: –*x* – 2, –*y* – 1, –*z* – 1).

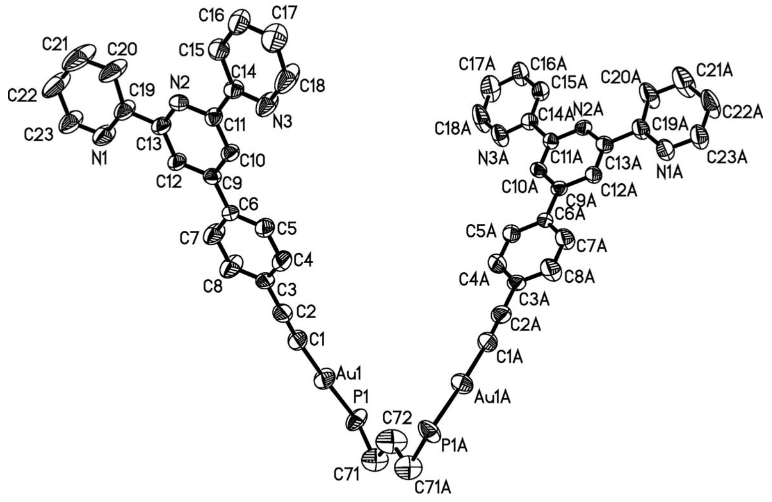

Figure 2. ORTEP drawing of **2**·2CH$_2$Cl$_2$ with atom labeling scheme showing 30% thermal ellipsoids. Phenyl rings of dppp, CH$_2$Cl$_2$ molecules, and hydrogen atoms are omitted for clarity (symmetry code for A: –*x* + 1, *y*, 0.5 – *z*).

These Au···Au distances are much longer than 3.6 Å,[11d] indicating no intramolecular or intermolecular Au···Au interaction in these complexes.

C–H···Au Interaction

Weak X–H···M hydrogen bonds have received much attention in recent years, and they could be structurally significant in constructing supramolecular architectures, especially when no other classical hydrogen bonds and M···M interactions exist in a structure.[14b,19b–19d] As the metal centers act as Lewis bases, the electron-rich metals such as late transition metals in low oxidation states are favored. The X–H···M interactions with angles less than 130° have generally been excluded.[15,21] In the crystal structure of **1**·2CH$_2$Cl$_2$, as shown in Figure 3, the molecules of **1** are linked through C14–H14A···Au (–*x* – 3, –*y* – 1, –*z*) ($d_{\mathrm{H}\cdots\mathrm{Au}}$ = 3.067 Å, ∠C–H···Au = 154.7°) and C27–H27A···Au (*x*, *y* + 1, *z*) ($d_{\mathrm{H}\cdots\mathrm{Au}}$ = 3.163 Å, ∠C–H···Au = 159.5°) interactions to produce 2-D layers, and the 2-D layers are reinforced through π···π stacking interactions occurring between two exactly parallel pyridine rings consisting of six atoms (N2, C6–C10) and its symmetric ring at the –*x* – 3, –*y* – 2, –*z* position [intercentroid distance 3.694(4) Å, perpendicular distance 3.486(3) Å, offset 1.222(3) Å]. Similar weak interaction has been observed in the crystal structure of [tpyC$_6$H$_4$C≡CAuPPh$_3$].[14b] The 2-D layers further interact with each other forming 3-D frameworks through C25–H25A···Cl1 (–*x* – 2, –*y*, –*z* – 1) weak hydrogen bonds [$d_{\mathrm{H}\cdots\mathrm{Cl}}$ = 2.820 Å, $d_{\mathrm{C25}\cdots\mathrm{Cl}}$ = 3.658 Å, ∠C25–H25A···Cl1 (–*x* – 2, –*y*, – *z* – 1) = 151°] and Cl2···Cl2 (–*x* – 3, –*y* – 1, –*z*, 3.129 Å) weak interactions (see Figure 4).[22] No obvious weak interaction was observed for **2**·2CH$_2$Cl$_2$.

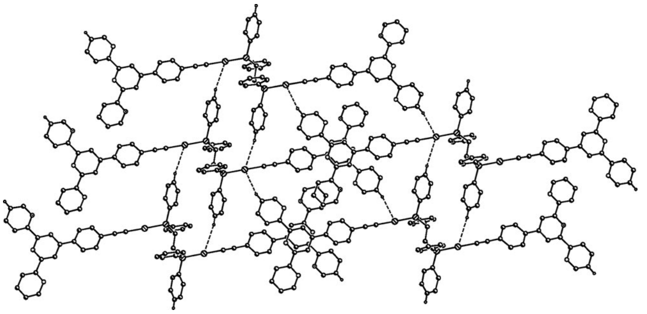

Figure 3. The 2-D layer of **1**·2CH$_2$Cl$_2$ induced by C–H···Au and π···π interactions. CH$_2$Cl$_2$ molecules and hydrogen atoms are omitted for clarity except H14A, H27A and their symmetrical atoms.

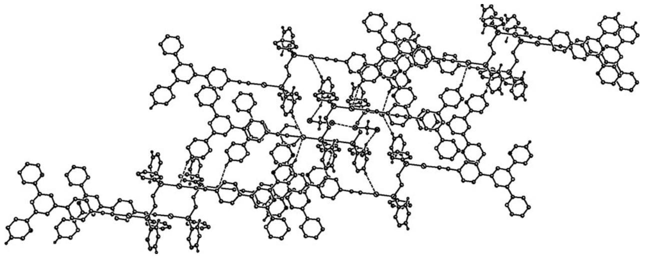

Figure 4. The 3-D framework of **1**·$2CH_2Cl_2$. Phenyl rings of dppe and most hydrogen atoms are omitted for clarity.

Photophysical Properties

Absorption Spectra

UV/Vis absorption data for **1**–**5** in dichloromethane solution at 298 K are summarized in Table 2. The corresponding electronic absorption spectra are depicted in Figure 5. Though the spacers between two P donors in the diphosphane ligands change, the absorption spectra of complexes **1**–**5** are similar throughout the series, and they all display two distinct and intense absorption bands with one maxima at ca. 232 nm, and the other at ca. 315 nm with a shoulder absorption at ca. 303 nm. By comparison with the corresponding absorptions of the complexes [Pt{$Ph_2P(CH_2)_n$-PPh_2}($C\equiv CC_6H_4$tpy)$_2$] (n = 1, 2, and 3) in our previous work and the analogous [tpy$C_6H_4C\equiv CAuPPh_3$] and [(tpy$C_6H_4C\equiv CAu)_2$(μ-dppd)] {dppd = 1,10-bis(diphenylphosphanyl)decane} complexes reported by the Vicente group,[6,14b] the former higher energy bands arise primarily from diphosphane-centered transitions, and the latter lower energy bands are mainly due to intraligand (IL) π→π* transitions of the $C\equiv CC_6H_4$tpy units, mixed probably with some Au orbital character. The low-energy absorption bands in complexes **1**–**5** display vibrational character with the vibronic spacings around 1257 cm^{-1}, corresponding to vibrational stretching frequencies of the pyridyl in $C\equiv CC_6H_4$tpy units.[6] In addition, complexes **1**–**5** exhibit large molar absorption coefficients (ε = 7.972×10^4 to 1.130×10^5), which reveals their strong light-absorbing ability.[6,7d]

Table 2. UV/Vis absorption data of **1**–**5** in dichloromethane solution at 298 K.

Compound	λ [nm] (ε [$M^{-1}cm^{-1}$])
1	232 (103500), 301 (90230), 315 (96660)
2	232 (99500), 303 (85910), 315 (90340)
3	232 (113000), 303 (93080), 316 (96310)
4	232 (94400), 303 (79720), 314 (82880)
5	232 (104500), 302 (89550), 314 (93580)

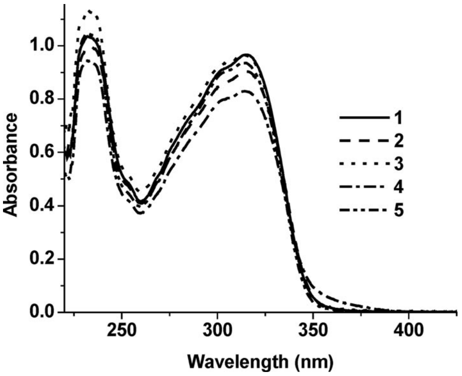

Figure 5. UV/Vis absorption spectra of **1**–**5** in dichloromethane solutions at 298 K.

Luminescence

The luminescence data, including emission wavelengths, lifetimes, and quantum yields of **1**–**5**, are presented in Table 3. The emission spectra of **1**–**5** in the solid state and in dichloromethane solution at 298 K are shown in Figures 6 and 7, respectively. All the dinuclear gold(I) complexes **1**–**5** exhibit dual emission bands both in the solid state and in dichloromethane solution at 298 K. Most low-energy bands for complexes **1**–**5** in the solid state and in the dichloromethane solution display vibronic character with spacings in the range of 1225–1339 cm^{-1} which is typical of the $\nu_{C\cdots C}$ and $\nu_{C\cdots N}$ aromatic vibrational modes in the alkynyl ligands.[6,14b] As no obvious π···π stacking and Au···Au interactions are observed in the crystal structure of complex **2** and the emission bands of complexes **1**–**5** are similar, the low energy emissions may arise from intraligand character. Compared with the emission spectrum of tpy$C_6H_4C\equiv CH$, together with consideration of the smaller Stokes' shifts,[6] the high-energy emissions of binuclear gold(I) complexes **1**–**5** arise most probably from the ^{1}(π→π*) excited state of the alkynyl ligand. With reference to the larger Stokes' shifts,[23] the vibrational spacings of typical $\nu_{C\cdots C}$ and $\nu_{C\cdots N}$ aromatic vibrational modes, and the emission properties of the reported gold(I)-alkynyl-phosphane complexes, especially those of [tpy$C_6H_4C\equiv CAuPPh_3$] and [(tpy$C_6H_4C\equiv CAu)_2$(μ-dppd)],[7d,11,14b] the low-energy emission bands at ca. 490–540 nm of complexes **1**–**5** are tentatively assigned to the ^{3}(π→π*) excited state of the acetylide ligand, mixed probably with some Au orbital character. In order to obtain deeper insight into the emissive properties, the radiation lifetime of the intense low-energy emission band at ca. 502 nm of complex **4** in dichloromethane solution was determined, and the long lifetime of 13.6 μs further proves the triplet parentage of the low-energy band.[6] It is worth noting that the lower energy emission band at ca. 502 nm of complex **4** in dichloromethane solution is more obvious, and it is red-shifted 7–11 nm relative to those of complexes **1**, **2**, **3**, and **5**, indicating that a stronger interaction between Au^I and the tpy$C_6H_4C\equiv C$ unit may exist in complex **4**, inducing stronger spin-orbital coupling and the increasing conjugated degree of the alkyne system. This can also be observed from the comparison between complex **1** and **2**. In complex **1**, the Au^I–C distance is 2.027(6) Å, a little longer (0.056 Å) than that of 1.971(12) Å in complex **2**, which indicates stronger interaction between Au^I and the tpy$C_6H_4C\equiv C$ unit in complex **2**, and the phosphorescence emission of complex **2** in dichloromethane solution is more obvious than that of complex **1**, and also a little red-shifted relative to that of complex **1**. In addition, the lower energy emission band at ca. 502 nm with a shoulder at 536 nm of complex **4** is close to that of 503 nm with a shoulder at 533 nm in [(tpy$C_6H_4C{\equiv}CAu)_2$(μ-dppd)], which is assigned to the intraligand $^3(\pi{\rightarrow}\pi^*)$ excited state of the acetylide ligand.[14b]

Table 3. Luminescence data of **1**–**5**.

Compound	λ_{em} [nm] (solid)	λ_{em} [nm] (τ_{em} [μs]) (CH_2Cl_2)	Φ_{em}[a]
1	393 sh, 418 505 sh, 540	374 492 (w)	0.1089[a]
2	394, 416 sh 505, 540 sh	377, 400 495 (w), 530 sh	0.0745[a]
3	395, 420 sh 510, 544 sh	375 494, 529sh	0.1419[a]
4	420 506, 540 sh	375 502 (13.6), 536 sh	0.1331[a]
5	398, 420 sh 511, 541 sh	373 491, 525	0.1340[a]

[a] The quantum yields in degassed CH_2Cl_2 are determined relative to that of $[Ru(bpy)_3](PF_6)_2$ (Φ = 0.062) in degassed CH_3CN.[24]

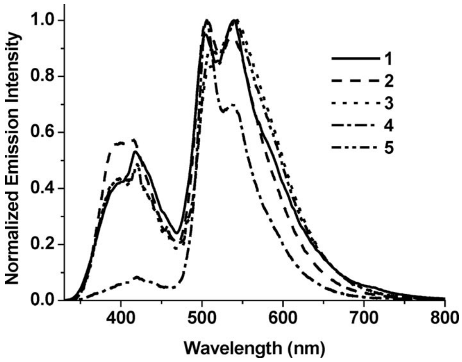

Figure 6. Emission spectra of **1**–**5** in the solid state at room temperature.

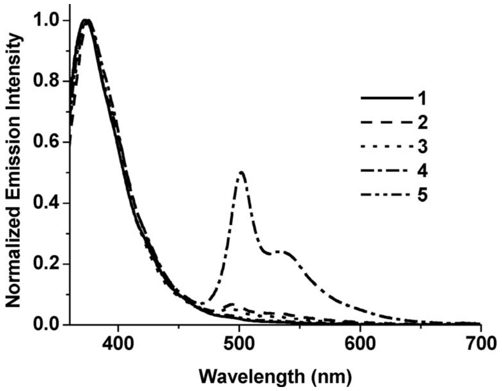

Figure 7. Emission spectra of **1**–**5** in fluid dichloromethane solution at room temperature.

Spectrophotometric Titration

Absorption Spectra Titration

The structural determination indicates the terpyridine units are free of coordination in complexes **1**·$2CH_2Cl_2$ and **2**·$2CH_2Cl_2$. These gold(I)-alkynyl-phosphane complexes can therefore be used as building blocks to react, through the polypyridine chelation, with Ln^{III} ions to form a Au_2Ln_2 array as reported in our previous work.[6] We have tried our best to synthesize the Au_2Ln_2 complexes, but no crystal suitable for single-crystal X-ray diffraction was obtained. So in order to explore how the UV/Vis absorption bands change when the dinuclear gold(I) complexes are coordinated to Ln^{III} ions, titrations were carried out by adding $Gd(hfac)_3(H_2O)_2$ to the dichloromethane solution of complex **1**. It must be mentioned that because significant dissociation often occurs in very diluted solutions,[8f] the original total concentrations of Au_2 units were kept at ca. 1.0×10^{-5} mol L^{-1} and those of $[Gd(hfac)_3(H_2O)_2]$ at ca. 2.0×10^{-5} mol L^{-1}. Figure 8 (a) shows that the absorbance increases little by little, following the gradual addition of the dichloromethane solution of $Gd(hfac)_3(H_2O)_2$ to that of **1**, and a graph of absorbance at 360 nm gives a smooth curve that fits well to a 2:1 binding ratio of Gd/Au_2 (Figure 8, b), which is similar to those of $[\{Pt(PPh_2(CH_2)_n\text{-}PPh_2)(C{\equiv}CC_6H_4tpy)_2\}\{Ln(hfac)_3\}_2]$ (n = 1, dppm; n = 2, dppe; n = 3, dppp; Ln = Eu, Nd, Yb) complexes in the previous work.[6]

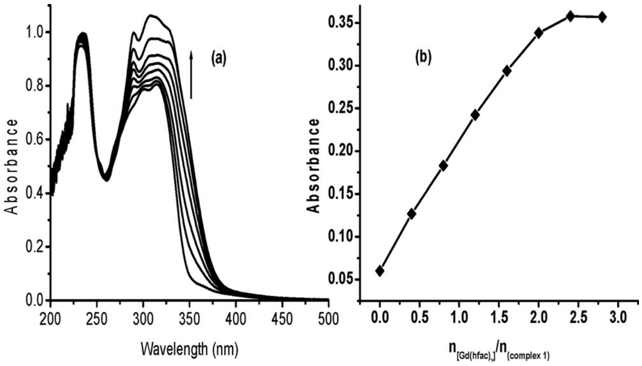

Figure 8. a: Changes in the UV/Vis absorption spectra by titration of **1** with $Gd(hfac)_3(H_2O)_2$ in dichloromethane. b: Changes of absorbance at 360 nm vs. the ratio of Gd to Au_2 moiety by titration of **1** with $Gd(hfac)_3(H_2O)_2$ in dichloromethane.

Luminescence Titration

For Ln^{III} complexes, both the singlet and triplet states of the ligand may transfer energy onto the Ln^{III} ions, but because of the short-lived character of the singlet state, energy transfer from it is often inefficient. So whether the energy gaps between the lowest triplets of the "metal complexes ligands" and Ln^{III} emitting levels are suitable for achieving sensitized luminescence of Ln^{III} is of primary importance. Though the triplet states of complexes **1**–**5** can not replace the triplet states of their corresponding Gd^{III} complexes, the easily determined triplet states of complexes **1**–**5** and their good luminescent properties at room temperature still make possible in a first step the following evaluations: (1) Whether complexes **1**–**5** can be used as sensitized chromophores for Ln^{III} luminescence; (2) which Ln^{III} ions may be more efficiently sensitized. For example, all the triplet states of complexes **1**–**5** in dichloromethane solution in the range of 18904–20367 cm^{-1} are lower than the emitting $^5D_4$ transition of Tb^{III} (20400 cm^{-1}) and are therefore not expected to sensitize Tb^{III} emission, but they all exceed to a sufficient extent the $^5D_0$ level at 17241 cm^{-1} (580 nm) of the corresponding Eu^{III} complexes (see Table 4), so it is possible to use complexes **1**–**5** as antenna chromophores to achieve the sensitized luminescence of Eu^{III} centers. In order to obtain more accurate data of the triplet states of the expected Au$_2$Ln$_2$ complexes, the luminescence of the Au$_2$Gd$_2$ dichloromethane solutions, which were prepared from complexes **1**–**5** and [Gd(hfac)$_3$(H$_2$O)$_2$] according to the corresponding 1:2 ratio, were determined without O$_2$. The lowest energy emitting state of Gd^{III}, at 32150 cm^{-1}, is too high to be excited by the antenna Au^I-alkynyl chromophores used in this study. Consequently, the emission spectra of the Gd^{III} complexes show exclusively Au^I-alkynyl-centered emission. The corresponding data are summarized in Table 4. Only the triplet states of **4**-Gd$_2$ can be observed at room temperature. The emission spectrum of **4**-Gd$_2$ in dichloromethane solution is depicted in Figure 9. The energy gap between the triplet state of **4**-Gd$_2$ at about 19342 cm^{-1} (517 nm) and the $^5D_0$ energy level of Eu^{III} is 2101 cm^{-1}, which is suitable for efficient energy transfer to Eu^{III} ions and prevention of possible energy back transfer.[25] Since complexes **1**–**5** are homologous, they are expected to behave as good energy donors to transfer energy to Eu^{III} centers effectively. In order to observe how the Eu^{III}-centered emission intensity changes when complexes **1**–**5** are coordinated to Eu(tta)$_3$, emission titrations were carried out in the aerated dichloromethane solutions. Upon excitation at 300–380 nm, the Eu^{III}-centered emission was enhanced greatly during the titration of [Eu(tta)$_3$(H$_2$O)$_2$] by adding different amounts of complex **1**, following the different Au$_2$/Eu ratios 0, 0.05, 0.10, 0.15, 0.20, 0.30, 0.40, and 0.50 (Figure 10). At a Au$_2$/Eu ratio higher than 0.50, the Eu^{III}-centered emission intensity decreased. The intensity of the Eu^{III}-centered emission at a Au$_2$/Eu ratio of 0.50 was 2.74-times that of [Eu(tta)$_3$(H$_2$O)$_2$]. This large enhancement confirms the energy transfer from the [(tpyC$_6$H$_4$C≡CAu)$_2$(μ-dppe)] unit to the Eu^{III} center effectively.

Table 4. Luminescence data of **1**-Ln$_2$ to **5**-Ln$_2$ solutions at 298 K.

Solution	λ_{em} [nm] (τ_{em} [μs]) (CH$_2$Cl$_2$)	Φ_{em}[a,b]
1-Eu$_2$	618 (600.7)	0.0446[a]
2-Eu$_2$	618 (612.1)	0.0407[a]
3-Eu$_2$	618 (610.6)	0.0440[a]
4-Eu$_2$	618 (606.9)	0.0405[a]
4-Gd$_2$	398, 420 sh 511, 541 sh	
5-Eu$_2$	618 (606.5)	0.0400[a]
1-Yb$_2$	980 (15.8)	0.0079[b]
2-Yb$_2$	980 (15.7)	0.0079[b]
3-Yb$_2$	980 (15.8)	0.0079[b]
4-Yb$_2$	980 (15.4)	0.0077[b]
5-Yb$_2$	980 (15.9)	0.0080[b]

[a] The quantum yields in degassed CH$_2$Cl$_2$ were determined relative to that of [Ru(bpy)$_3$](PF$_6$)$_2$ (Φ = 0.062) in degassed CH$_3$CN.[24] [b] The quantum yields of Yb^{III} complexes in dichloromethane solution at 298 K were estimated by the equation $\Phi = \tau_{obs}/\tau_0$, in which τ_{obs} is the observed emission lifetime and τ_0 is the radiative or "natural" lifetime of 2 ms. All the solutions containing Eu, Gd, and Yb were prepared from complexes **1** and [Eu(tta)$_3$(H$_2$O)$_2$], [Gd(hfac)$_3$(H$_2$O)$_2$], and [Yb(hfac)$_3$(H$_2$O)$_2$] according to the corresponding ratio 1:2.

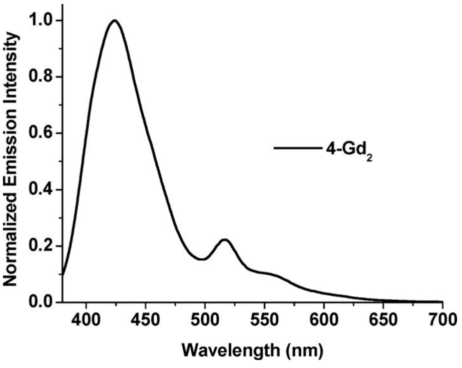

Figure 9. The emission spectrum of **4**-Gd$_2$ in dichloromethane solution at 298 K.

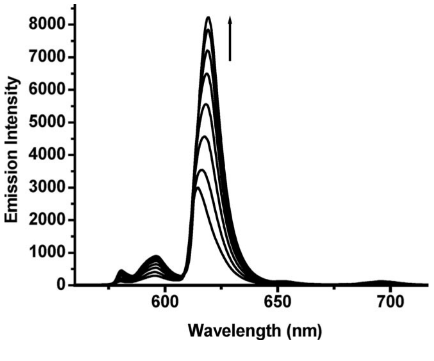

Figure 10. Changes in Eu^{III}-centered emission intensity upon titration of Eu(tta)$_3$(H$_2$O)$_2$ with complex **1** in dichloromethane upon excitation with 300 nm.

The maximum excitation wavelength of Eu^{III}-centered emission increased following the addition of [Eu(tta)$_3$(H$_2$O)$_2$] to the dichloromethane solution of complex **1**, however it did not increase again when the Eu/Au$_2$ ratio was ca. 2.0 (Figure S1), confirming the 1:2 binding ratio between complex **1** and Eu(tta)$_3$. The Eu^{III}-centered emission quantum yields of **1**-Eu$_2$ to **5**-Eu$_2$ in dichloromethane solutions fall in the range 0.0400–0.0472, which is similar to those (0.0373–0.0445) of mononuclear Pt^{II}-phosphane-alkynyl-Eu^{III} complexes of the same alkyne ligand tpyC$_6$H$_4$C≡CH,[6] further confirming that the efficient energy transfer occurred from the [(tpyC$_6$H$_4$C≡CAu)$_2$(μ-Ph$_2$P(CH$_2$)$_x$PPh$_2$)] (x = 2–6) series of units to the Eu^{III} centers. The luminescence data, including emission wavelengths, lifetimes, and quantum yields of **1**-Ln$_2$ to **5**-Ln$_2$, are presented in Table 4. All the Eu^{III} solutions exhibit characteristic emission bands of Eu^{III} ions at about 580, 596, 618, 652, and 695 nm for **1**-Eu$_2$ to **5**-Eu$_2$ solutions (prepared from [Eu(tta)$_3$(H$_2$O)$_2$] and complexes **1**–**5** according to a 2:1 ratio) corresponding to the transitions $^5D_0 \rightarrow {}^7F_0$, $^7F_1$, $^7F_2$, $^7F_3$, $^7F_4$, respectively, with the dominant band at 618 nm (Figure S2).

Upon titration of [$Yb(hfac)_3(H_2O)_2$] with complex **1** in dichloromethane solution, a dramatic enhancement of Yb^{III} emission was observed with the Au_2/Yb ratios changing from 0, 0.10, 0.20, 0.30, 0.40 to 0.50 (Figure 11), which indicates that efficient energy transfer occurs from the Au_2-alkynyl unit to Yb^{III} centers. The intensity of Yb^{III}-centered emission at ca. 980 nm with the Au_2/Yb ratio at 0.50 was 3.37-times that of [$Yb(hfac)_3(H_2O)_2$]. All the Au_2Yb_2 solutions (prepared from [$Yb(hfac)_3(H_2O)_2$] and complexes **1**–**5** according to a 2:1 ratio) exhibit the characteristic emission bands of Yb^{III} corresponding to the $^2F_{5/2}\rightarrow{}^2F_{7/2}$ transition at ca. 980 nm. The intrinsic quantum yields of Yb^{III} emission may be estimated by $\Phi = \tau_{obs}/\tau_0$, where τ_{obs} is the observed emission lifetime and τ_0 is the "natural lifetime".[6] The Au_2Yb_2 solutions show emission lifetimes from 14.6–15.9 µs and intrinsic quantum yields from 0.0073–0.0080 (see Table 4), which are comparable to those (0.0073–0.0080) of Pt^{II}-phosphane-alkynyl-Yb^{III} complexes of the same alkyne ligand $tpyC_6H_4C{\equiv}CH$ in our previous work.[6]

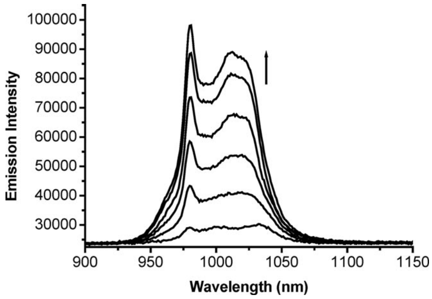

Figure 11. Changes of the Yb^{III}-centered emission intensity upon titration of $Yb(hfac)_3(H_2O)_2$ with complex **1** in dichloromethane upon excitation with 330 nm.

Conclusions

In conclusion, a series of dual luminescent binuclear gold(I) complexes of terpyridyl-functionalized alkyne ligands have been synthesized. Spectrophotometric titration and the quantum yields of Ln^{III} demonstrate that they can behave as good energy donors for sensitization of Eu^{III} and Yb^{III} emission, and as efficient chromophores, they are comparable to those of Pt^{II} complexes.[6]

Experimental Section

Materials and Reagents: The reagents 1,2-bis(diphenylphosphanyl)ethane (dppe), 1,3-bis(diphenylphosphanyl)propane (dppp), 1,4-bis(diphenylphosphanyl)butane (dppb), 1,5-bis(diphenylphosphanyl)pentane (dpppen), 1,6-bis(diphenylphosphanyl)hexane (dpph), tetrahydrothiophene (tht), and $H_3[AuCl_4]$ were commercially available without further purification. 4′-[4-{2-(trimethylsilyl)-1-ethynyl}phenyl]-2,2′:6′,2′′-terpyridine ($tpyC_6H_4C{\equiv}CTMS$), $(tpyC_6H_4C{\equiv}CAu)_n$, [$Eu(tta)_3(H_2O)_2$], and [$Ln(hfac)_3(H_2O)_2$] (Ln = Gd, Yb) were prepared by the published methods.[26,7d,27] All solvents were purified and distilled using standard procedures before use except those for spectroscopic measurements which were of spectroscopic grade. All other reagents were of analytical grade and were used as received.

Preparation of Complexes: All reactions were carried out under dry argon using Schlenk techniques at room temperature and a vacuum-line system unless specified.

[$(tpyC_6H_4C{\equiv}CAu)_2$(µ-dppe)] (1): Dppe (20.3 mg, 98%, 0.050 mmol) was added to a dichloromethane (15 mL) solution of $(tpyC_6H_4C{\equiv}CAu)_n$ (52.9 mg, 0.10 mmol) with stirring at room temperature for 30 min. The solution was concentrated and the product was purified by chromatography on a short silica-gel column using dichloromethane/methanol (100:2) as eluent. Addition of *n*-hexane to the concentrated solution gave the product as a pale yellow powder (yield 45 mg, 62%). Pale yellow crystals were obtained by layering *n*-hexane onto the concentrated dichloromethane solution in the absence of light. $C_{72}H_{52}Au_2N_6P_2{\cdot}CH_2Cl_2$ (1542.06): calcd. C 56.87, H 3.53, N 5.45; found C 56.57, H 3.59, N 5.36. ESI-MS: *m/z* (%) = 1457.4 $[M + H]^+$, 1124.7 $[M - tpyC_6H_4C{\equiv}C]^+$. ^1H NMR ($CDCl_3$): δ = 8.75–8.72 (m, 8 H, $tpyC_6H_4C{\equiv}C$), 8.67 (d, $^3J_{HH}$ = 8.0 Hz, 4 H, H3′), 7.90–7.85 (m, 8 H, $tpyC_6H_4C{\equiv}C$), 7.72–7.66 (m, 12 H, $tpyC_6H_4C{\equiv}C$ and PPh_2), 7.53–7.51 (m, 12 H, PPh_2), 7.35 (m, 4 H, H5′), 2.70 (s, 4 H, CH_2) ppm. IR spectrum (KBr): $\tilde{\nu}$ = 2110 [m (C≡C)] cm^{-1}.

[$(tpyC_6H_4C{\equiv}CAu)_2$(µ-dppp)] (2): This compound was prepared by the same synthetic procedure as that of **1** except for using dppp instead of dppe. Color: pale yellow, yield: 43 mg, 59%. Pale yellow crystals were obtained by layering *n*-hexane onto the concentrated dichloromethane solution in the absence of light. $C_{73}H_{54}Au_2N_6P_2$ (1471.15): calcd. C 59.58, H 3.70, N 5.71; found C 59.63, H 3.77, N 5.69. ESI-MS: *m/z* (%) = 1471.3 $[M + H]^+$, 1138.2 $[M - C_6H_4C{\equiv}C]^+$. ^1H NMR ($CDCl_3$): δ = 8.74–8.72 (m, 8 H, H3 and H6′), 8.67 (d, $^3J_{HH}$ = 8.0 Hz, 4 H, H3′), 7.87 (td, $^3J_{HH}$ = 8.0, $^4J_{HH}$ = 2.0 Hz, 4 H, H4′), 7.84 (d, *J* = 7.2 Hz, 4 H, $tpyC_6H_4C{\equiv}C$), 7.77–7.72 (m, 8 H, $tpyC_6H_4C{\equiv}C$ and PPh_2), 7.65–7.63 (m, 4 H, PPh_2), 7.49–7.44 (m, 12 H, PPh_2), 7.34 (m, 4 H, H5′), 2.87 (m, *J* = 4.5 Hz, 4 H, PCH_2), 1.99 (m, 2 H, PCH_2CH_2) ppm. IR spectrum (KBr): $\tilde{\nu}$ = 2110 [m (C≡C)] cm^{-1}.

[$(tpyC_6H_4C{\equiv}CAu)_2$(µ-dppb)] (3): This compound was prepared by the same synthetic procedure as that of **1** except for using dppb instead of dppe. Color: pale yellow, yield: 45 mg, 61%. $C_{74}H_{56}Au_2N_6P_2$ (1485.18): calcd. C 59.82, H 3.80, N 5.66; found C 59.52, H 3.85, N 5.60. ESI-MS: *m/z* (%) = 1152.1 $[M - tpyC_6H_4C{\equiv}C]^+$. ^1H NMR ($CDCl_3$): δ = 8.74–8.72 (m, 8 H, H3 and H6′), 8.67 (d, $^3J_{HH}$ = 8.0 Hz, 4 H, H3′), 7.87 (td, $^3J_{HH}$ = 7.6, $^4J_{HH}$ = 2.0 Hz, 4 H, H4′), 7.84 (d, *J* = 8.0 Hz, 4 H, $tpyC_6H_4C{\equiv}C$), 7.71–7.63 (m, 12 H, $tpyC_6H_4C{\equiv}C$ and PPh_2), 7.50–7.49 (m, 12 H, PPh_2), 7.35 (ddd, $^3J_{HH}$ = 8.0 and 4.8, $^4J_{HH}$ = 1.2 Hz, 4 H, H5′), 2.44 (m, 4 H, PCH_2), 1.83 (m, 4 H, PCH_2CH_2) ppm. IR spectrum (KBr): $\tilde{\nu}$ = 2110 [m (C≡C)] cm^{-1}.

[$(tpyC_6H_4C{\equiv}CAu)_2$(µ-dpppen)] (4): This compound was prepared by the same synthetic procedure as that of **1** except for using dpppen instead of dppe. Color: pale yellow, yield: 48 mg, 64%. $C_{75}H_{58}Au_2N_6P_2$ (1499.21): calcd. C 60.07, H 3.90, N 5.61; found C 59.86, H 3.96, N 5.65. ESI-MS: *m/z* (%) = 1166.5 $[M - tpyC_6H_4C{\equiv}C]^+$. ^1H NMR ($CDCl_3$): δ = 8.73–8.72 (m, 8 H, H3 and H6′), 8.66 (d, $^3J_{HH}$ = 8.0 Hz, 4 H, H3′), 7.87 (td, $^3J_{HH}$ = 7.6, $^4J_{HH}$ = 2.0 Hz, 4 H, H4′), 7.85 (d, *J* = 8.0 Hz, 4 H, $tpyC_6H_4C{\equiv}C$), 7.74–7.64 (m, 12 H, $tpyC_6H_4C{\equiv}C$ and PPh_2), 7.49–7.46 (m, 12 H, PPh_2), 7.35 (ddd, $^3J_{HH}$ = 7.6 and 4.8, $^4J_{HH}$ = 1.2 Hz, 4 H, H5′), 2.41 (m, *J* = 6.0 Hz, 4 H, PCH_2), 1.69 [s, 6 H, $PCH_2(CH_2)_3$] ppm. IR spectrum (KBr): $\tilde{\nu}$ = 2109 [m (C≡C)] cm^{-1}.

[$(tpyC_6H_4C{\equiv}CAu)_2$(µ-dpph)] (5): This compound was prepared by the same synthetic procedure as that of **1** except for using dpph instead of dppe. Color: pale yellow, yield: 76 mg, 90%. $C_{76}H_{60}Au_2N_6P_2$ (1513.23): calcd. C 60.30, H 4.00, N 5.56; found C 60.01, H 4.03, N 5.47. ESI-MS: *m/z* (%) = 1180.9 [M – tpy$C_6H_4C{\equiv}C$]$^+$. ^1H NMR ($CDCl_3$): δ = 8.73–8.72 (m, 8 H, H3 and H6′), 8.66 (d, $^3J_{HH}$ = 8.0 Hz, 4 H, H3′), 7.87 (td, $^3J_{HH}$ = 7.8, $^4J_{HH}$ = 2.0 Hz, 4 H, H4′), 7.83 (d, *J* = 8.4 Hz, 4 H, tpy$C_6H_4C{\equiv}C$),7.72–7.63 (m, 12 H, tpy$C_6H_4C{\equiv}C$ and P*Ph*$_2$), 7.49–7.46 (m, 12 H, P*Ph*$_2$), 7.35 (ddd, $^3J_{HH}$ = 7.6 and 4.8, $^4J_{HH}$ = 1.2 Hz, 4 H, H5′), 2.43 (m, *J* = 7.5 Hz, 4 H, PCH_2), 1.60 (s, 4 H, PCH_2CH_2) ppm. 1.48 (m, 4 H, $PCH_2CH_2CH_2$). IR spectrum (KBr): $\tilde{\nu}$ = 2111 [m (C≡C)] cm^{-1}.

Crystal Structure Determination: Crystals suitable for X-ray diffraction studies of **1**·$2CH_2Cl_2$, and **2**·$2CH_2Cl_2$ were obtained by layering *n*-hexane onto the corresponding dichloromethane solution in the absence of light. Single crystals were sealed in capillaries with mother liquors. **1**·$2CH_2Cl_2$ and **2**·$2CH_2Cl_2$ were measured with a RIGAKU MERCURY CCD and RIGAKU SCXmini diffractometer, respectively, using the ω-scan technique at room temperature with graphite-monochromated Mo-K_α radiation (λ = 0.71073 Å). The CrystalClear software package[28–29] and Bruker SAINT[30] were used for data reduction and empirical absorption correction, respectively. The structures were solved by direct methods. The heavy atoms were located from the E-map, and the rest of the non-hydrogen atoms were found in subsequent Fourier maps. The non-hydrogen atoms were refined anisotropically, whereas the hydrogen atoms were generated geometrically with isotropic thermal parameters. The structures were refined on F^2 by full-matrix least-squares methods using the SHELXTL-97 program package.[31] The crystallographic data of **1**·$2CH_2Cl_2$ and **2**·$2CH_2Cl_2$ are summarized in Table 1.

CCDC-770767 (for **1**·$2CH_2Cl_2$) and CCDC-770768 (for **2**·CH_2Cl_2) contain the supplementary crystallographic data for this paper. These data can be obtained free of charge from The Cambridge Crystallographic Data Centre via www.ccdc.cam.ac.uk/data_request/cif.

Physical Measurements: ^1H NMR spectra were measured with a Bruker Avance III (400 MHz) spectrometer with $SiMe_4$ as the internal reference. Infrared (IR) spectra were obtained from KBr pellets using a Bruker Optics TENSOR 27 FT-IR spectrophotometer. UV/Vis absorption spectra were recorded with a Purkinje General TU-1901 UV/Vis spectrophotometer. Elemental analyses (C, H, N) were carried out with a Perkin–Elmer model 240C elemental analyzer. Electrospray mass spectra (ES-MS) were performed with a Finnigan LCQ mass spectrometer using a dichloromethane/methanol mixture as the mobile phase. Steady-state excitation and emission spectra in the UV/Vis region were recorded with a Perkin–Elmer LS55 luminescence spectrometer with a red-sensitive photomultiplier type R928 or an Edinburgh F900 fluorescence spectrometer. The steady-state near-infrared (NIR) emission spectra were measured with an Edinburgh FLS920 fluorescence spectrometer equipped with a Hamamatsu R5509–72 supercooled photomultiplier tube at 193 K and a TM300 emission monochromator with NIR grating blazed at 1000 nm. The NIR emission spectra were corrected via a calibration curve supplied with the instrument. Emission lifetimes were determined with an Edinburgh Analytical Instrument (F900 fluorescence spectrometer) and the resulting emission was detected by a thermoelectrically cooled Hamamatsu R3809 photomultiplier tube. The emission quantum yields (Φ) in the UV/Vis region in degassed dichloromethane solutions at room temperature were calculated by $\Phi_s = \Phi_r(B_r/B_s)(ns/n_r)^2(D_s/D_r)$ using $[Ru(bpy)_3](PF_6)_2$ in acetonitrile as the standard (Φ_{em} = 0.062), where the subscripts r and s denote reference standard and the sample solution, respectively; and *n*, *D* and Φ are the refractive index of the solvents, the integrated intensity and the luminescence quantum yield, respectively.[24,32] The quantity *B* in the equation $\Phi_s = \Phi_r(B_r/B_s)(ns/n_r)^2(D_s/D_r)$ is calculated by $B = 1–10^{-AL}$, where *A* is the absorbance at the excitation wavelength and *L* is the optical path length. All the solutions used for determination of emission lifetimes and quantum yields were prepared after rigorous removal of oxygen by three successive freeze–pump–thaw cycles under vacuum in a 10-cm^3 round-bottomed flask equipped with a side arm 1-cm fluorescence cuvette and sealed from the atmosphere by a quick-release Teflon® stopper.[6b]

Supporting Information (see also the footnote on the first page of this article): Changes of the excitation spectra and the maximum excitation wavelength with the emission at 618 nm upon titration of complex **1** with $[Eu(tta)_3(H_2O)_2]$ in dichloromethane following different Eu/Au$_2$ ratios (Figure S1), and Eu^{III}-centered emission spectra of **1**-Eu$_2$ in dichloromethane solution (Figure S2).

Acknowledgments

This work was supported financially by the National Natural Science Foundation of China (NSFC) (20801047, 20931006, and 20772103), the Foundation of Xuzhou Normal University (07XLA07, KY2007039, and XGG2007034) and the QingLan Project of Jiangsu Province (08QLT001).

---

[1] a) J. C. G. Bünzli, *Acc. Chem. Res.* **2006**, *39*, 53–61; b) J. C. G. Bünzli, C. Piguet, *Chem. Soc. Rev.* **2005**, *34*, 1048–1077; c) J. C. G. Bünzli, C. Piguet, *Chem. Rev.* **2002**, *102*, 1897–1928.

[2] a) Z. N. Chen, Y. Fan, J. Ni, *Dalton Trans.* **2008**, 573–581; b) M. D. Ward, *Coord. Chem. Rev.* **2007**, *251*, 1663–1677; c) J. G. Mao, *Coord. Chem. Rev.* **2007**, *251*, 1493–1520; d) D. Parker, *Coord. Chem. Rev.* **2000**, *205*, 109–130; e) K. Kuriki, Y. Koike, Y. Okamoto, *Chem. Rev.* **2002**, *102*, 2347–2356; f) A. de Bettencourt-Dias, *Dalton Trans.* **2007**, 2229–2241.

[3] a) Z. Zheng, *Chem. Commun.* **2001**, 2521–2529; b) F. X. Zang, Z. R. Hong, W. L. Li, M. T. Li, X. Y. Sun, *Appl. Phys. Lett.* **2004**, *84*, 2679–2681; c) D. Guo, C. Y. Duan, F. Lu, Y. Hasegawa, Q. J. Meng, S. Yanagida, *Chem. Commun.* **2004**, 1486–1487; d) X. Zhu, J. Lü, X. Li, S. Gao, G. Li, F. Xiao, R. Cao, *Cryst. Growth Des.* **2008**, *8*, 1897–1901.

[4] a) T. Lazarides, N. M. Tart, D. Sykes, S. Faulkner, A. Barbieri, M. D. Ward, *Dalton Trans.* **2009**, 3971–3979; b) T. Lazarides, H. Adams, D. Sykes, S. Faulkner, G. Calogero, M. D. Ward, *Dalton Trans.* **2008**, 691–698; c) S. G. Baca, H. Adams, D. Sykes, S. Faulkner, M. D. Ward, *Dalton Trans.* **2007**, 2419–2430; d) F. Kennedy, N. M. Shavaleev, T. Koullourou, Z. R. Bell, J. C. Jeffery, S. Faulkner, M. D. Ward, *Dalton Trans.* **2007**, 1492–1499; e) T. Lazarides, M. A. H. Alamiry, H. Adams, S. J. A. Pope, S. Faulkner, J. A. Weinstein, M. D. Ward, *Dalton Trans.* **2007**, 1484–1491; f) T. K. Ronson, H. Adams, L. P. Harding, S. J. A. Pope, D. Sykes, S. Faulkner, M. D. Ward, *Dalton Trans.* **2007**, 1006–1022.

[5] a) A. P. S. Samuel, E. G. Moore, M. Melchior, J. Xu, K. N. Raymond, *Inorg. Chem.* **2008**, *47*, 7535–7544; b) M. Giraud, E. S. Andreiadis, A. S. Fisyuk, R. Demadrille, J. Pécaut, D. Imbert, M. Mazzanti, *Inorg. Chem.* **2008**, *47*, 3952–3954; c) C. P. Montgomery, B. S. Murray, J. N. Elizabeth, R. Pal, D. Parker, *Acc. Chem. Res.* **2009**, *42*, 925–937; d) E. G. Moore, A. P. S. Samuel, K. N. Raymond, *Acc. Chem. Res.* **2009**, *42*, 542–552; e) J. L. Worlinsky, S. Basu, *J. Phys. Chem. B* **2009**, *113*, 865–868; f) K. Hanaoka, K. Kikuchi, S. Kobayashi, T. Nagano, *J. Am. Chem. Soc.* **2007**, *129*, 13502–13509; g) H. Li, P. Liu, Y. Wang, L. Zhang, J. Yu, H. Zhang, B. Liu, U. Schubert, *J. Phys. Chem. C* **2009**, *113*, 3945–3949.

[6] a) X. L. Li, F. R. Dai, L. Y. Zhang, Y. M. Zhu, Q. Peng, Z. N. Chen, *Organometallics* **2007**, *26*, 4483–4490; b) X. L. Li, L. X.

Shi, L. Y. Zhang, H. M. Wen, Z. N. Chen, *Inorg. Chem.* **2007**, *46*, 10892–10900.

[7] a) H. B. Xu, L. X. Shi, E. Ma, L. Y. Zhang, Q. H. Wei, Z. N. Chen, *Chem. Commun.* **2006**, 1601–1603; b) H. B. Xu, L. Y. Zhang, Z. L. Xie, E. Ma, Z. N. Chen, *Chem. Commun.* **2007**, 2744–2746; c) H. B. Xu, L. Y. Zhang, Z. H. Chen, L. X. Shi, Z. N. Chen, *Dalton Trans.* **2008**, 4664–4670; d) H. B. Xu, L. Y. Zhang, J. Ni, H. Y. Chao, Z. N. Chen, *Inorg. Chem.* **2008**, *47*, 10744–10752.

[8] a) T. K. Ronson, T. Lazarides, H. Adams, S. J. A. Pope, D. Sykes, S. Faulkner, S. J. Coles, M. B. Hursthouse, W. Clegg, R. W. Harrington, M. D. Ward, *Chem. Eur. J.* **2006**, *12*, 9299–9313; b) P. D. Beer, F. Szemes, P. Passaniti, M. Maestri, *Inorg. Chem.* **2004**, *43*, 3965–3975; c) S. I. Klink, H. Keizer, F. C. J. M. van Veggel, *Angew. Chem. Int. Ed.* **2000**, *39*, 4319–4321; d) N. M. Shavaleev, L. P. Moorcraft, S. J. A. Pope, Z. R. Bell, S. Faulkner, M. D. Ward, *Chem. Eur. J.* **2003**, *9*, 5283–5291; e) N. M. Shavaleev, L. P. Moorcraft, S. J. A. Pope, Z. R. Bell, S. Faulkner, M. D. Ward, *Chem. Commun.* **2003**, 1134–1135; f) N. M. Shavaleev, G. Accorsi, D. Virgili, Z. R. Bell, T. Lazarides, G. Calogero, N. Armaroli, M. D. Ward, *Inorg. Chem.* **2005**, *44*, 61–72.

[9] a) F. F. Chen, Z. Q. Bian, Z. W. Liu, D. B. Nie, Z. Q. Chen, C. H. Huang, *Inorg. Chem.* **2008**, *47*, 2507–2513; b) M. Shi, F. Li, T. Yi, D. Zhang, H. Hu, C. Huang, *Inorg. Chem.* **2005**, *44*, 8929–8936; c) H. Xin, M. Shi, X. C. Gao, Y. Y. Huang, Z. L. Gong, D. B. Nie, H. Cao, Z. Q. Bian, F. Y. Li, H. H. Chun, *J. Phys. Chem. B* **2004**, *108*, 10796–10800; d) H. Xin, M. Shi, X. M. Zhang, F. Y. Li, Z. Q. Bian, K. Ibrahim, F. Q. Liu, H. H. Chun, *Chem. Mater.* **2003**, *15*, 3728–3733.

[10] a) M. Latva, H. Takalo, V.-M. Mukkala, C. Matachescu, J. C. Rodriguez-Ubis, J. Kankare, *J. Lumin.* **1997**, *75*, 149–169; b) N. M. Shavaleev, R. Scopelliti, F. Gumy, J. C. G. Bünzli, *Inorg. Chem.* **2009**, *48*, 6178–6191; c) D. S. Oxley, R. W. Walters, J. E. Copenhafer, T. Y. Meyer, S. Petoud, H. M. Edenborn, *Inorg. Chem.* **2009**, *48*, 6332–6334.

[11] a) W. Lu, N. Zhu, C. M. Che, *J. Am. Chem. Soc.* **2003**, *125*, 16081–16088; b) C. M. Che, H.-Y. Chao, V. M. Miskowski, Y. Li, K. K. Cheung, *J. Am. Chem. Soc.* **2001**, *123*, 4985–4991; c) W. Lu, H. F. Xiang, N. Zhu, C. M. Che, *Organometallics* **2002**, *21*, 2343–2346; d) H. Y. Chao, W. Lu, Y. Li, M. C. W. Chan, C. M. Che, K. K. Cheung, N. Zhu, *J. Am. Chem. Soc.* **2002**, *124*, 14696–14706.

[12] a) X. X. Lu, C. K. Li, E. C. C. Cheng, N. Y. Zhu, V. W. W. Yam, *Inorg. Chem.* **2004**, *43*, 2225–2227; b) V. W. W. Yam, S. W. K. Choi, K. K. Cheung, *Organometallics* **1996**, *15*, 1734–1739.

[13] P. Li, B. Ahrens, A. D. Bond, J. E. Davies, O. F. Koentjoro, P. R. Raithby, S. J. Teat, *Dalton Trans.* **2008**, 1635–1646.

[14] a) W. J. Hunks, M. A. MacDonald, M. C. Jennings, P. J. Puddephatt, *Organometallics* **2000**, *19*, 5063–5070; b) J. Vicente, J. Gil-Rubio, N. Barquero, P. G. Jones, D. Bautista, *Organometallics* **2008**, *27*, 646–659.

[15] J. Vicente, M. T. Chicote, M. M. Alvarez-Falcón, *Organometallics* **2005**, *24*, 5956–5963.

[16] S. S. Y. Chui, M. F. Y. Ng, C. M. Che, *Chem. Eur. J.* **2005**, *11*, 1739–1749.

[17] M. A. MacDonald, R. J. Puddephatt, G. P. A. Yap, *Organometallics* **2000**, *19*, 2194–2199.

[18] a) V. W. W. Yam, S. K. Yip, L. H. Yuan, K. L. Cheung, K. K. Cheung, *Organometallics* **2003**, *22*, 2630–2637; b) H. S. Tang, N. Zhu, V. W. W. Yam, *Organometallics* **2007**, *26*, 22–25; c) X. He, N. Zhu, V. W. W. Yam, *Organometallics* **2009**, *28*, 3621–3624.

[19] a) J. Vicente, M. T. Chicote, M. M. Álvarez-Falcón, P. G. Jones, *Organometallics* **2005**, *24*, 2764–2772; b) J. Vicente, M. T. Chicote, M. M. Álvarez-Falcón, P. G. Jones, *Organometallics* **2005**, *24*, 4666–4675; c) J. Vicente, M. T. Chicote, M. M. Álvarez-Falcón, M. A. Fox, D. Bautista, *Organometallics* **2003**, *22*, 4792–4797; d) J. Vicente, M. T. Chicote, M. M. Álvarez-Falcon, P. G. Jones, *Chem. Commun.* **2004**, 2658–2659.

[20] a) C. P. McArdle, S. Van, M. C. Jennings, R. J. Puddephatt, *J. Am. Chem. Soc.* **2002**, *124*, 3959–3965; b) N. C. Habermehl, M. C. Jennings, C. P. McArdle, F. Mohr, R. J. Puddephatt, *Organometallics* **2005**, *24*, 5004–5014; c) C. P. McArdle, M. J. Irwin, M. C. Jennings, J. J. Vittal, R. J. Puddephatt, *Chem. Eur. J.* **2002**, *8*, 723–734; d) C. P. McArdle, M. C. Jennings, J. J. Vittal, R. J. Puddephatt, *Chem. Eur. J.* **2001**, *7*, 3572–3583; e) M. J. Irwin, J. J. Vittal, R. J. Puddephatt, *Organometallics* **1997**, *16*, 3541–3547; f) G. Jia, R. J. Puddephatt, I. D. Scott, J. Vittal, *Organometallics* **1993**, *12*, 3565–3574.

[21] J. Vicente, M.-T. Chicote, M. D. Abrisqueta, M. M. Alvarez-Falcón, *Organometallics* **2003**, *22*, 4327–4333.

[22] E. M. Barranco, O. Crespo, M. C. Gimeno, A. Laguna, *Inorg. Chem.* **2000**, *39*, 680–687.

[23] a) D. H. Waldeck, *Chem. Rev.* **1991**, *91*, 415–436; b) K. Haskins-Glusac, I. Ghiviriga, K. A. Abbound, K. S. Schanze, *J. Phys. Chem. B* **2004**, *108*, 4969–4978.

[24] J. N. Demas, G. A. Crosby, *J. Phys. Chem.* **1971**, *75*, 991–1024.

[25] L. N. Puntus, K. A. Lyssenko, M. Y. Antipin, J. C. Bunzli, *Inorg. Chem.* **2008**, *47*, 11095–11107.

[26] V. Grosshenny, F. M. Romero, R. Ziessel, *J. Org. Chem.* **1997**, *62*, 1491–1500.

[27] Y. Hasegawa, Y. Kimura, K. Murakoshi, Y. Wada, J. H. Kim, N. Nakashima, T. Yamanaka, S. Yanagida, *J. Phys. Chem.* **1996**, *100*, 10201–10205.

[28] Rigaku & Molecular Structure Corporation, *CrystalClear*, Rigaku Corporation, Tokyo, Japan, and MSC, The Woodlands, Texas, USA, **2000**.

[29] Rigaku, *CrystalClear*, Rigaku Corporation, Tokyo, Japan, **2005**.

[30] *Bruker SAINT*, Bruker AXS Inc., Madison, Wisconsin, USA, **2001**.

[31] G. M. Sheldrick, *SHELXL-97*, *Program for the Refinement of Crystal Structures*, University of Göttingen, Göttingen, Germany, **1997**.

[32] J. V. Caspar, T. J. Meyer, *J. Am. Chem. Soc.* **1983**, *105*, 5583–5590.

Received: March 24, 2010